Composite Hierarchical Pitch Angle Control for a Tidal Turbine Based on the Uncertainty and Disturbance Estimator

Xiuxing Yin and Xiaowei Zhao

***Abstract*—With the fast development of tidal turbines for sustainable energy generations, reliable and efficient tidal pitch systems are highly demanded. This paper presents a systematic design for a novel tidal pitch system based on hydraulic servo and bevel geared transmission. This system holds the characteristics of compact and triangular structure, making it easy to be installed in a narrow turbine hub. The pitch system dynamics are modelled by taking account of model uncertainties and external disturbances. An uncertainty and disturbance estimator (UDE)-based robust pitch control algorithm is developed to achieve effective pitch angle regulation, disturbance rejection and generator power smoothing. The UDE controller is designed in a composite hierarchical manner that includes an upper level power smoothing controller and a low level pitch angle tracking controller. The performance of the proposed pitch system and the UDE control is demonstrated through extensive simulation studies based on a 600 kW tidal turbine under varying tidal speeds. Compared with the conventional controller, the UDE based pitch controller can achieve more reliable power smoothing and pitch angle tracking with higher accuracy.**

***Index Terms*—Tidal turbine; Pitch system; Power smoothing; Pitch angle tracking; UDE based pitch control.**

Nomenclature

$\boldsymbol{A}_m \in \Re^{3\times3}, \boldsymbol{B}_m \in \Re^{3\times1}$ the constant matrices of the reference model

$\boldsymbol{A}_p \in \Re^{3\times3}, \boldsymbol{B}_p \in \Re^{3\times1}, \boldsymbol{C}_p \in \Re^{3\times1}$ the state matrices of the hydraulic pitch servo

$\boldsymbol{B}_p^+$ the Moore-Penrose inverse of $\boldsymbol{B}_p$

b a known control gain

$\hat{b}$ the control gain estimate

$\tilde{b}$ the estimation error $\tilde{b} = b - \hat{b}$

b_L an equivalent viscous damping coefficient in the geared transmission

b_{ls} damping ratio of the low-speed side

b_β a known control gain for the pitch angle

$c(t)$ a piecewise uniformly and continuous bounded command

C_p the power coefficient of the tidal turbine

c_1 to c_6 the coefficients for calculating C_p

c_m the total leakage coefficient of the hydraulic pitch servo

$C(s)$ the Laplace transforms of $c(t)$

$d(x,t)$ the lumped non-affine term including uncertainties and disturbances

$d_p(t)$ the lumped uncertain and disturbance term

$\hat{d}_p(t)$ the estimate of $d_p(t)$

d_β the lumped unknown disturbance and model uncertainties

D_m the constant displacement of the hydraulic motor

$\boldsymbol{e}_p(t)$ pitch angle tracking error

$\boldsymbol{E}_p(s)$ the Laplace transforms of $\boldsymbol{e}_p(t)$

e_β the bounded pitch angle deviation or tracking error

$g(x)$ a known smooth nonlinear function

$G_f(s)$ a strictly proper stable low-pass filter

$g_f(t)$ the impulse response of the filter $G_f(s)$

$g_\beta(\omega_g, v, \beta)$ a known smooth nonlinear function

i_p the bevel gear transmission ratio

$\boldsymbol{I} \in \Re^{3\times3}$ an identity matrix

J_b the inertia of the turbine blades

J_g the inertia of the generator

J_m the pitch servo side inertia

J_t the turbine rotational inertia

$\boldsymbol{K}_2 \in \Re^{3\times3}$ an error feedback gain matrix

K_c the flow-pressure coefficient

k_{ls} the equivalent spring stiffness

k_g the damping coefficient of the high speed shaft

K_q the pitch servo valve flow gain coefficient

K_u the constant proportional mapping gain

k_t damping coefficient

$L^{-1}\{\bullet\}$ the inverse Laplace operation of $\bullet$

$\boldsymbol{P}$ an adequately selected positive definite matrix

p_L the load pressure of the hydraulic pitch servo

This work was supported by the UK Engineering and Physical Sciences Research Council under grant EP/R007470/1. Xiuxing Yin and Xiaowei Zhao (corresponding author) are with the School of Engineering, the University of Warwick, Coventry, CV4 7AL, U. K. Emails: x.yin.2@warwick.ac.uk, xiaowei.zhao@warwick.ac.uk.

q_L the hydraulic load flow rate
R the tidal turbine blade radius
s the Laplace operator
T_e the magnetic reaction torque of the generator
T_h the high speed shaft torque
T_L the low-speed shaft side reaction torque
T_m the torque from the hydraulic pitch servo
T_p the total inertia moment acting on the turbine blades
v the effective tidal stream speed
$V_1(t)$, $V_2(t)$ Lyapunov function candidates
V_p the total motor volume of the hydraulic pitch servo
x the state variable of generator power
$\boldsymbol{x}_m$ the reference state vector
$\boldsymbol{x}_p$ the state vector of the hydraulic pitch servo
$\boldsymbol{X}_p(s)$ the Laplace transform of x_p
x_v the pitch servo valve spool displacement
β the tidal blade pitch angle
β_e the hydraulic fluid's effective volume elasticity modulus
β_r the reference pitch angle control input
γ_1, γ_2 positive constants
δ_m the un-modelled dynamics and parametric uncertainties
ρ the seawater density (1025 kg/m^3)
θ_t the angular deviation of the turbine rotor
θ_{ls} the angular deviation of the low speed shaft
θ_m the rotation angle of the servo side bevel gear
λ the tidal turbine tip speed ratio (TSR)
λ_i an intermediate variable
$\lambda_{\min}(\bullet)$ and $\lambda_{\max}(\bullet)$ the minimum and maximum eigenvalues of the given matrix $\bullet$
τ a small time constant
ω_{ls} the angular rotation speed of the low speed shaft
ω_g the rotation speed of the generator
ω_t the rotation speed of the turbine rotor
$\Delta d_p = d_p(t) - \hat{d}_p(t)$ the estimation error of the lumped disturbance term $d_p(t)$
$\|\bullet\|$ the matrix Frobenius norm for a given matrix $\bullet$
* the convolution operator

I. Introduction

As a promising renewable energy source with high predictability, tidal energy is gaining increased attention and is becoming more and more competitive with other energy sources such as wind, wave and solar in terms of resource availability, supply security and reliability. Tidal turbines exploit tidal stream flows directly without the need of large civil engineering structures to build up a water head. Their design and development have increased significantly in recent years. A number of full-scale turbine prototypes have been developed or are scheduled to be deployed, such as the 300 kW MCT technology, the 1 MW twin rotor system in UK [1], the contra-rotating 500 kW TidEl turbines [2], the DeltaStream Turbine [3] and the Lunar Energy tidal turbine [4].

However, the harsh and highly turbulent working conditions pose a major challenge to the tidal turbines regarding the reliability, effectiveness and survivability. Thus, advanced technologies or subsystems that can effectively tackle these problems, which therefore reduce tidal turbines' operation and maintenance costs, are of significant importance. One such subsystem is the blade pitch system which has been widely used in modern wind turbines [5], [6] and has been proven to be a reliable and cost effective technology for power smoothing and load mitigation. Similarly, tidal turbines can benefit from pitch control. The pitch system can pitch the blades to fully utilize bi-directional tidal flows, to limit power generations when the tidal speed is above rated and to achieve hydrodynamic stall in case of emergence. However, so far very few research have been conducted on the pitch systems of tidal turbines while pitch system technology of wind turbines are not suitable to be directly applied for tidal turbines due to inherent differences of both systems e.g., different stall and loading characteristics since seawater is about 800 times denser than air.

A hydraulic pitch control mechanism was described in [7] for a straight-bladed Darrieus type vertical-axis tidal turbine. The movement of the pitch mechanism is of sinusoidal shape and is continuously variable in amplitude. The blade pitch actuation is powered by the turbine's own rotation and is thus passively regulated. In [8] and [9], a collective pitch system was designed for tidal turbine using a rack and pinion gear set and hydraulic drive to provide an available blade pitch angle. Then a reduced variation pitch control strategy was proposed based on tidal current velocity preview to reduce pitch actions and extend the tidal turbine's working life. Comparative results validated the significant reductions of pitch actions and relatively high efficiency for energy generation. In [10], a pitch angle controller for a variable-speed tidal turbine was developed and the performance comparison between the pitch regulated tidal turbine and a stall regulated tidal turbine was examined in MATLAB under turbulent tidal flows. The results indicated that the pitch regulated turbines was a more attractive solution for turbine developers. The rack and pinion set is a conveniently used mechanism to convert rotary motions into linear motions and vice versa, holding the advantages of being cheap and compact. However, the most adverse disadvantages of rack and pinion would be the inherent frictions and low mass moment of inertia since the rack and pinion can only work with certain levels of friction and will be subject to wear more than usual during long-time linear and rotary motion transformations [11]. Thus, for the rack and pinion type pitch systems, the motion transformations are inevitably imprecise, leading to inaccurate pitch actuation. Some of the existing designs of the tidal turbine pitch subsystem are bought from wind turbines which are relatively common and simple. Hence,

there is a need for advanced and robust pitch system to deliver more precise pitch control actions and simultaneously take into account the particular characteristics of tidal turbines.

In this paper, a novel and effective tidal pitch system is proposed in which hydraulic servo and bevel geared transmission are employed to highly enhance the pitch control accuracy. The tidal pitch system has compact and stable structure, and is readily sized and installed into the front inner narrow space of the turbine hub. The excellent characteristic of the bevel geared transmission can also guarantee smooth and direct pitch actions. The dynamic characteristics of the pitch system is modelled and analyzed, and external loads and disturbances are also considered and integrated into the overall system model. An efficient and robust UDE based pitch control scheme is then designed. The UDE control has been successfully applied to a wide class of linear, nonlinear uncertain systems and is easy to be implemented and tuned while offering better robust performances than the traditional control schemes [12]. It includes 3 inherent design freedoms: a reference model, an error feedback gain and a filter, which enables high decoupling between reference tracking and disturbance rejection [13]. The UDE based robust control is also able to achieve good robust performance by estimating and compensating the unknown dynamics and disturbances in a system with a filter having the appropriate frequency characteristics [14]. The UDE based pitch control scheme is designed in a composite hierarchical manner that includes an upper level generator power smoothing controller and a low level pitch angle tracking controller. The main contributions and novelty of this paper are highlighted as follows.

(a) A novel and effective tidal pitch system is proposed based on hydraulic servo and bevel geared transmission.

(b) An efficient and robust UDE based pitch control scheme is designed in a composite hierarchical manner that includes an upper level generator power smoothing controller and a low level pitch angle tracking controller. The overall stability of the UDE pitch control is proved through Lyapunov functions.

(c) The dynamics and control performances of the proposed pitch system and UDE pitch controller are demonstrated through extensive simulations based on a 600 kW tidal turbine under both the normal and extreme conditions.

The remainder of this paper is organized as follows: In Section II, the design of the proposed tidal pitch system is introduced. In section III, dynamics modelling of the proposed pitch system is presented. Section IV presents the UDE based power smoothing control of the tidal turbine. Section V presents the UDE based pitch angle control. Section VI illustrates the stability analysis of the overall UDE pitch controller. Section VII presents the validations and discussions of the proposed pitch system and UDE controller. Section VIII concludes the paper.

II The Tidal Pitch System

The novel tidal pitch system is designed for a general variable-speed, three-bladed, horizontal axis tidal turbine to provide accurate and bidirectional pitch actions based on hydraulic servo and bevel geared transmission. As illustrated in Fig. 1, the pitch system mainly consists of a hydraulic pitch servo 1, a servo side bevel gear 2, blade side bevel gears 3, pitch bearings 4 and auxiliary support 6. The hydraulic pitch servo 1 is installed in the front inner cone of the turbine hub and is rigidly connected to the servo side bevel gear 2. The three blade side bevel gears 3 are connected to blade roots through bolts and pitch bearings 4, and are also precisely engaged with the servo side bevel gear 2. Thus, the three turbine blades can be uniformly pitched by the hydraulic pitch servo 1 through the bevel gears 2, 3 and pitch bearings 4. The blade pitch angle is determined by the rotation angle of the pitch servo and the transmission ratio of the bevel gears. The auxiliary support 6 includes some specific structures such as waterproof sealing and housing to support the pitch system.

Since the hydraulic servo has relatively high torque/volume ratio, the pitch system can be adequately and compactly sized into the inner narrow space of the turbine hub. The pitch system is also designed as a triangular structure with large stability and a low center of gravity for operations. This design is essentially different from the aforementioned pitch systems and effectively satisfies the special requirements of fast dynamic performances, precise pitch motions and large pitch torques of tidal turbines.

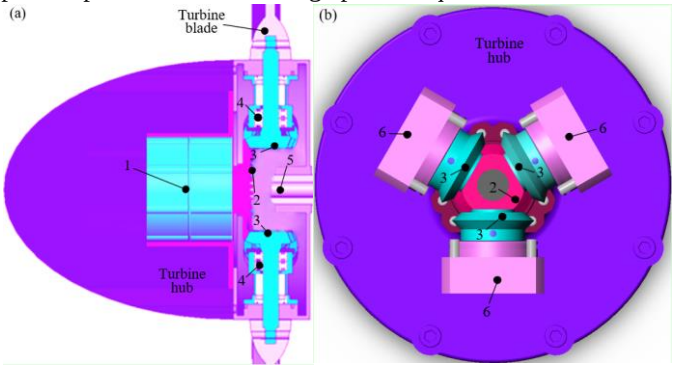

1-The hydraulic pitch servo 2-The servo side bevel gear 3-The blade side bevel gear 4-Pitch bearing 5-The main shaft 6-Auxiliary support

Fig. 1 Design of the novel tidal pitch system

As shown schematically in Fig. 2, the hydraulic pitch servo mainly consists of a servo motor, a hydraulic pump, check valves, a servo valve, a high pressure accumulator (HPA), a low pressure accumulator (LPA), a relief valve, a hydraulic motor and a UDE pitch angle controller. The servo motor drives the hydraulic pump to supply high pressure hydraulic oil flow, which is then routed by the check valves and the servo valve to the hydraulic motor that is rigidly connected to the bevel gears to generate pitch motions. The pump in the turbine hub is adjustable from full to a 50% flow rate, and its efficiency only slightly changes with time-varying tidal flow speeds. The accumulators, HPA and LPA function as energy storage in terms of compressed gas to provide filter pressure pulsations and pressure compensations. The HPA is used to maintain a sufficiently high pressure in the suction ports of the hydraulic machines. The relief valve is designed for limiting the hydraulic system pressure and ensuring system safety in case of large pitch torque pulsations, by setting the safety pressure at 10–20% above the maximum operation pressure [15].

The servo valve with matched orifices is controlled by the

UDE pitch controller to accurately regulate the direction, rotation angle and speed of the hydraulic motor that consequently drives the bevel gears fixed at the blade roots to change blade pitch angles accordingly. The pitch angle controller generates control commands for the servo valve based on the feedback pitch angles and thus the blades are pitched corresponding to different tidal speed conditions. In case of emergency, the tidal turbine can be stopped by pitching the blades to feather and using high pressure flows from the HPA. The designed pitch system is robust against various exogenous disturbances due to the inherent loading balance and high pressure limitations of the hydraulic transmission.

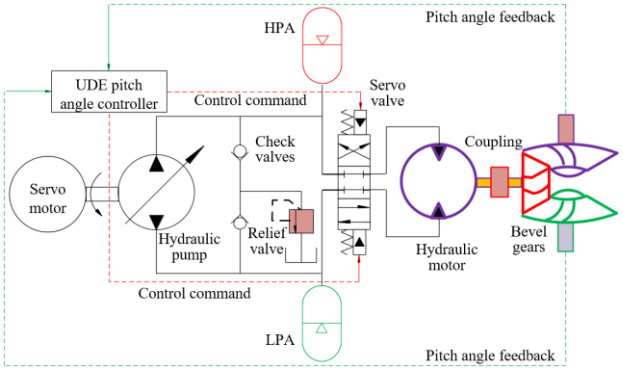

Fig. 2 Design of the hydraulic pitch servo

Since the seawater density is around 800 times higher than air, generating the same amount of power requires much smaller sized tidal turbines than wind turbines. Therefore, significantly different from wind turbine pitch systems that do not stress much on turbine size to accommodate, the proposed tidal pitch system design takes into account the much smaller tidal turbine hub size. It is designed based on compact hydraulic servo and bevel geared transmission with triangular structure such that it can be adequately and compactly sized into the inner narrow space of the turbine hub. The employed hydraulic servo based tidal pitch system not only has relatively higher torque/volume ratio, but also is much sturdier than the commonly used electric motor based pitch systems in wind turbines. In addition this tidal pitch design makes the tidal turbine durable enough to survive the hostile underwater environment. In addition, the tidal pitch angle range is much smaller than that of wind turbines due to the much higher seawater density, which requires higher accuracies on the tidal pitch system and its control than its wind turbine counterpart.

III. Dynamics Modelling

The dynamics of the tidal pitch system can be modelled based on fundamental governing equations of each component in an integrated configuration. External loads and environmental conditions that can alter the operation characteristics of the pitch system will also be considered and integrated into the overall system model.

A. Hydrodynamics of the Tidal Turbine

The hydrodynamic torque and tidal stream speed acting on the tidal turbine blades can be represented as

$$\begin{cases} T_t = \dfrac{\rho\pi R^5 \omega_t^2 C_p}{2\lambda^3} \\ v = \dfrac{\omega_t R}{\lambda} \end{cases} \tag{1}$$

As indicated in (1), the tidal turbine torque is strongly dependent on both the power coefficient C_p and TSR (tip-speed ratio), which are expressed as

$$\begin{cases} C_p(\lambda,\beta) = c_1\left(\dfrac{c_2}{\lambda_i} - c_3\beta - c_4\right)\exp(-\dfrac{c_5}{\lambda_i}) + c_6\lambda \\ \lambda_i = \dfrac{1}{\lambda + 0.08\beta} - \dfrac{0.035}{\beta^3 + 1} \end{cases} \tag{2}$$

where the constant coefficients c_1 to c_6 are: c_1 = 0.5176, c_2 = 116, c_3 = 0.4, c_4 = 5, c_5 = 21 and c_6 = 0.0068.

The $C_p - (\lambda, \beta)$ characteristics for different values of the pitch angle β are shown in Fig. 3, which implies that the maximum value of C_p ($C_{p\max}$ = 0.4798) is achieved when β = 0° and λ = 8. With the increasing pitch angle from 0° to 15° and TSR from 0 to 9, the power coefficient decreases from 0.48 to around 0.1. Hence the turbine power generations can be readily regulated at stable values by maintaining the optimal blade pitch angle when the tidal stream is above rated speed.

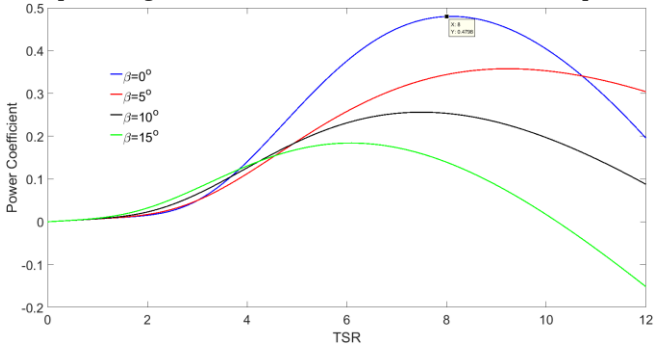

Fig. 3 The typical power coefficient curves for a tidal turbine

B. The Tidal Turbine Drivetrain

As the turbine rotor spins, the mechanical energy of the rotor is transmitted via the drivetrain to the generator where the tidal energy is converted into the electricity. As illustrated in Fig. 4, the equivalent geared drivetrain of the tidal turbine consists of a small mass and a large lumped mass that represent the inertias of the generator rotor and the turbine rotor. A geared transmission with ratio i_g is placed between the masses for increasing the turbine speed and decreasing the torque.

The turbine side dynamics is represented as

$$\begin{cases} J_t\dot{\omega}_t = T_t - k_t\omega_t - T_L \\ T_L = k_{ls}(\theta_t - \theta_{ls}) + b_{ls}(\omega_t - \omega_{ls}) \end{cases} \tag{3}$$

The generator side dynamics is represented as

$$J_g\dot{\omega}_g = T_h - k_g\omega_g - T_e \tag{4}$$

The geared transmission that links the low speed shaft and high speed shaft can be described as

$$\begin{cases} T_L\omega_{ls} = T_h\omega_g \\ \dfrac{\omega_g}{\omega_{ls}} = \dfrac{T_L}{T_h} = i_g \end{cases} \tag{5}$$

Considering (3) and (5), the turbine rotation speed is

$$\begin{cases} \omega_t = \Delta\omega_t + \omega_{ls} = \Delta\omega_t + \dfrac{\omega_g}{i_g} \\ \Delta\omega_t = \omega_t - \omega_{ls} \end{cases} \tag{6}$$

Substituting (5) and (6) into (3) gives

$$J_t\left(\Delta\dot{\omega}_t + \frac{\dot{\omega}_g}{i_g}\right) = T_t - k_t\omega_t - T_h \cdot i_g \tag{7}$$

Substituting $T_h = J_g\dot{\omega}_g + k_g\omega_g + T_e$ from (4) into (7) gives

$$\dot{\omega}_g = \frac{i_g}{J_t + J_g i_g^2}T_t - \frac{\left(k_t + k_g i_g^2\right)}{J_t + J_g i_g^2}\omega_g - \frac{i_g^2}{J_t + J_g i_g^2}T_e - \frac{i_g\left(k_t\Delta\omega_t + J_t\Delta\dot{\omega}_t\right)}{J_t + J_g i_g^2} \tag{8}$$

Substituting (1) and (2) into (8) and rearranging the resulting equations yields

$$\dot{\omega}_g = g_\beta\left(\omega_g, \beta\right) + b_\beta\beta + d_\beta \tag{9}$$

$$\begin{cases} g_\beta\left(\omega_g,\beta\right) = \dfrac{\rho\pi R^5\omega_t^2 i_g}{2\lambda^3\left(J_t + J_g i_g^2\right)}\left[c_1\left(\dfrac{c_2}{\lambda_i} - c_4\right)\exp\left(-\dfrac{c_5}{\lambda_i}\right) + c_6\lambda\right] \\ \quad -\dfrac{\left(k_t + k_g i_g^2\right)}{J_t + J_g i_g^2}\omega_g - \dfrac{i_g^2}{J_t + J_g i_g^2}T_e \\ b_\beta = -\dfrac{\rho\pi R^5\omega_t^2 i_g c_1 c_3\exp\left(-\dfrac{c_5}{\lambda_i}\right)i_g}{2\lambda^3\left(J_t + J_g i_g^2\right)} \\ d_\beta = -\dfrac{i_g\left(k_t\Delta\omega_t + J_t\Delta\dot{\omega}_t\right)}{J_t + J_g i_g^2} \end{cases} \tag{10}$$

As expressed in (10), the generator torque T_e is attainable from the generator side converter regulations and is thus assumed known for the pitch angle controller while the disturbance term b_β consists of shaft angle and speed deviations, which is the main source of decreasing the drivetrain transmission efficiency over a wide power range.

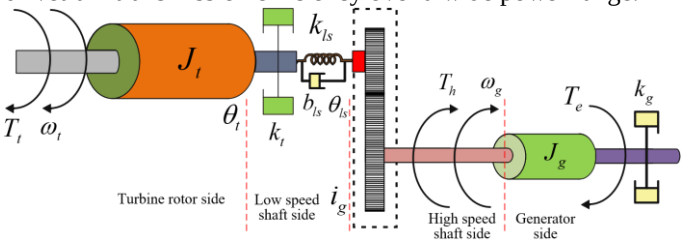

Fig. 4 Schematic of the geared drivetrain

C. The Bevel Geared Transmission

The dynamic torque balance equation for the bevel geared transmission is described as

$$\begin{cases} T_m = \left(J_m + \dfrac{J_b}{i_p^2}\right)\ddot{\theta}_m + b_L\dot{\theta}_m + \dfrac{T_p}{i_p} \\ \theta_m = \beta \cdot i_p \end{cases} \tag{11}$$

The actual pitch load T_p depends on the aerofoil shapes of the turbine blades and blade pitch angle, and can thus be as an out-plane torques that induce the fore-aft motions of the blades and hub. The pitch load can also be calculated by using similar equations as wind turbines [16].

D. The Pitch Servo System

As mentioned earlier in section II and Fig. 2, the hydraulic pitch servo system is controlled by a four-way electrohydraulic servo-valve which consists of two inlet and two outlet orifices and a spool that changes the flow passage area of the outlet orifices. The control flow equation of the hydraulic servo valve for the load flow rate is written as

$$q_L = K_q x_v - K_c p_L \tag{12}$$

The servo valve dynamics is sufficiently faster than the dynamics of the rest parts of the system. Therefore the servo-valve opening is directly related to the control input u by a known constant proportional mapping.

$$x_v = K_u \cdot u \tag{13}$$

The governing equation of the flow-pressure continuous model of the hydraulic motor relates the pressure differential across the hydraulic motor chambers and the passage area to the flow rate. Thus,

$$q_L = D_m\dot{\theta}_m + c_m p_L + \frac{V_p}{4\beta_e}\dot{p}_L \tag{14}$$

The active torque generated by the hydraulic motor is

$$T_m = D_m p_L + \delta_m \tag{15}$$

The state-space representation of the hydraulic wind power system is derived by combining (11)-(15) as follows

$$\dot{\boldsymbol{x}}_p = \boldsymbol{A}_p\boldsymbol{x}_p + \boldsymbol{B}_p u + \boldsymbol{C}_p d_p(t) \tag{16}$$

The hydraulic pitch servo is in principle a servo system represented by a state space model (17). The un-modelled dynamics and parametric uncertainties are represented as disturbance term in (17).

$$\begin{cases} \boldsymbol{A}_p = \begin{bmatrix} 0 & 1 & 0 \\ 0 & -\dfrac{b_L}{J_{mb}} & \dfrac{D_m}{J_{mb}i_p} \\ 0 & -\dfrac{4\beta_e D_m i_p}{V_p} & -\dfrac{4\beta_e K_{cm}}{V_p} \end{bmatrix}, \boldsymbol{B}_p = \begin{bmatrix} 0 \\ 0 \\ \dfrac{4\beta_e K_q K_u}{V_p} \end{bmatrix}; \\ \boldsymbol{C}_p = \begin{bmatrix} 0 \\ 1 \\ 0 \end{bmatrix}, J_{mb} = J_m + \dfrac{J_b}{i_p^2}; K_{cm} = K_c + c_m. \end{cases} \tag{17}$$

IV. Power Smoothing Control of The Tidal Turbine

The tidal pitch control is designed in a composite hierarchical manner that includes an upper level generator power smoothing controller and a low level pitch angle tracking controller. It operates when the tidal speed is above rated. The generator power smoothing controller is designed to generate a suitable reference pitch angle that is employed to maintain the generator power at the rated value. In this section, an UDE-based robust power smoothing controller is proposed, which can handle of model nonlinearity, uncertainty and system disturbances. Due to the introductions of extra control parameters, UDE filter and error feedback gain, it enables effective disturbance rejection and can effectively handle model uncertainty [17].

A. Controller Synthesis

The generator output power is expressed as $P_g = T_e\omega_g$. Since $\ell_{b_\beta}P_g \neq 0$ (ℓ denotes the Lie derivative), the relative degree of generator power output is 1. Hence the dynamics of the generator power can be formulated based on (9) as follows

$$\begin{cases} \dot{P}_g = \ell_{g_\beta} P_g + \ell_{b_\beta} P_g \beta + \ell_{d_\beta} P_g + \dot{T}_e \omega_g \\ \ell_{g_\beta} P_g = g_\beta T_e; \ell_{b_\beta} P_g = b_\beta T_e; \ell_{d_\beta} P_g = d_\beta T_e. \end{cases} \tag{18}$$

And the generator power dynamics is written as

$$\begin{cases} \dot{x} = g(x) + b\beta + d(x,t) \\ x = P_g, g(x) = \ell_{g_\beta} P_g; \\ b = \ell_{b_\beta} P_g; d(x,t) = \ell_{d_\beta} P_g + \dot{T}_e \omega_g \end{cases} \tag{19}$$

With the generator power dynamics developed in (19), the UDE-based power smoothing controller is synthesized with the control objective that the output power x asymptotically tracks the rated generator power x_r as closely as possible in spite of various model uncertainties and disturbances. The control input of the pitch angle is produced based on the tracking error between actual and the rated generator power.

The power tracking error is written as

$$e = x_r - x \tag{20}$$

The desired error dynamics is designed as

$$\dot{e} = -K_1 e \tag{21}$$

Combining (19), (20) and (21) gives

$$\dot{e} = \dot{x}_r - \dot{x} = \dot{x}_r - g(x) - b\beta - d(x,t) = -K_1 e \tag{22}$$

According to the system dynamics in (19), the uncertain term $d(x,t)$ can be estimated by using a filter with appropriate bandwidth as follows

$$\begin{aligned} \hat{d}(x,t) &= d(x,t) * g_f(t) = (\dot{x} - g(x) - b\beta) * g_f(t) \\ &= L^{-1}\{G_f(s)\} * (\dot{x} - g(x) - b\beta) \end{aligned} \tag{23}$$

The low-pass filter $G_f(s)$ is expressed as

$$G_f(s) = \frac{1}{1+\tau s} \tag{24}$$

Assuming the estimation error as $\Delta d = d(x,t) - \hat{d}(x,t)$ and combining (22) and (23) yield

$$b\beta = \dot{x}_r - g(x) - L^{-1}\{G_f(s)\} * (\dot{x} - g(x) - b\beta) + K_1 e - \Delta d \tag{25}$$

Following the procedures in [18], re-arranging (25) leads to the UDE control design as follows

$$\beta = b^{-1}\left\{ L^{-1}\left[\frac{1}{1-G_f(s)}\right] * (\dot{x}_r + K_1 e) - g(x) - L^{-1}\left[\frac{sG_f(s)}{1-G_f(s)}\right] * x \right\} \tag{26}$$

Since the rated generator power is assumed as a constant, $\dot{x}_r = 0$ and the following equations are derived based on (24).

$$\begin{cases} \dfrac{1}{1-G_f(s)} = 1 + \dfrac{1}{\tau s}; \\ \dfrac{sG_f(s)}{1-G_f(s)} = \dfrac{1}{\tau}. \end{cases} \tag{27}$$

Then the control law in (26) is written as

$$\beta = b^{-1}\left\{ K_1 e - g(x) - \frac{1}{\tau}\left[e + K_1 \int e(\xi) \mathrm{d}\xi \right] \right\} \tag{28}$$

The control law in (28) has two parts: a model compensation term for canceling the known system dynamics and a local positive feedback loop behaving like a Proportional–Integral (PI) controller. The error feedback gain can be chosen arbitrarily large to attenuate the high-frequency components of the uncertainty and disturbances. It is worth noting that the control gain b also needs to be calculated by using the control input, which may lead to algebraic loop during the control implementations. A practical solution to this problem is to use the control input at previous time instants to compute the control gain at the current time instant when the sampling rate in the digital implementation is chosen highly faster than the variation rate of the control input.

B. Estimation of Tidal Stream Speeds

The control law in (28) is implemented assuming that all the states and the tidal stream speed are available for feedback. However, in practice, the tidal stream speed is not always directly measurable or is very expensive to measure. Thus the UDE controller (28) adopts an estimation of the tidal speed signal to construct the control law.

Assuming an ideal drivetrain model, i.e. $\Delta\omega_t = \Delta\dot{\omega}_t = 0$, the turbine torque is estimated based on (8) as follows

$$\hat{T}_t = L^{-1}\{G_f(s)\} * \left\{ \left(\frac{J_t}{i_g} + J_g i_g \right) \dot{\omega}_g + \left(\frac{k_t}{i_g} + k_g i_g \right) \omega_g + T_e \cdot i_g \right\} \tag{29}$$

By re-arranging (1), the turbine torque is also represented as

$$\hat{T}_t = \frac{\rho \pi R^2 \hat{v}^3 i_g C_p}{2\omega_g} \tag{30}$$

Thus the tidal stream speed is readily estimated as

$$\hat{v} = \left(\frac{2\omega_g \hat{T}_t}{\rho \pi R^2 i_g C_p} \right)^{\frac{1}{3}} \tag{31}$$

As indicated in (31), the estimation of tidal stream speeds needs the information of power coefficient C_p that depends on the blade pitch angle and TSR, and is thus not always known at the current time instant. A practical solution to this problem is to use the power coefficient C_p calculated at a previous time instant to calculate the tidal stream speed at the current time instant since the tidal turbine power coefficient changes much slower than the turbine pitch system and tidal streams. In addition, the calculation in (31) can also be made accurate enough when the sampling rate in the online digital implementation is chosen highly faster than the variation rate of the power coefficient. Then the UDE-based robust control law for power smoothing in (28) can be re-formulated as

$$\beta = \hat{b}^{-1}\left\{ K_1 e - g(x) - \frac{1}{\tau}\left[e + K_1 \int e(\xi) \mathrm{d}\xi \right] \right\} \tag{32}$$

Actually the pitch servo system may not accurately achieve the reference or the desired pitch angle in (32) due to the servo performance limitations. The pitch angle control law in (32) should be rewritten as the desired or the reference pitch angle

$$\beta_r = \hat{b}^{-1}\left\{ K_1 e - g(x) - \frac{1}{\tau}\left[e + K_1 \int e(\xi) \mathrm{d}\xi \right] \right\} \tag{33}$$

where β is rearranged as β_r and $\beta_r = \beta + e_\beta$.

V. PITCH ANGLE CONTROL

In this section, the UDE based pitch angle controller is designed based on (16) to have the pitch servo system to asymptotically track the derived reference pitch angle trajectory in (33) as closely as possible, while the uncertainty and disturbance are completely compensated and rejected.

In order for the closed-loop pitch servo system to satisfy the desired pitch angle tracking performances, the following stable reference model in a controllable canonical is selected

$$\dot{\boldsymbol{x}}_m = \boldsymbol{A}_m \boldsymbol{x}_m + \boldsymbol{B}_m c(t) \tag{34}$$

The control objective is thus to track the reference state vector $\boldsymbol{x}_m$ and the tracking error $\boldsymbol{e}_p(t) = \boldsymbol{x}_m - \boldsymbol{x}_p$ satisfies the ideal dynamics

$$\dot{\boldsymbol{e}}_p(t) = (\boldsymbol{A}_m + \boldsymbol{K}_2)\boldsymbol{e}_p(t) \tag{35}$$

Combining (16), (34), and (35) results in

$$\boldsymbol{B}_p u = \boldsymbol{A}_m \boldsymbol{x}_p + \boldsymbol{B}_m c(t) - \boldsymbol{A}_p \boldsymbol{x}_p - \boldsymbol{K}_2 \boldsymbol{e}_p(t) - \boldsymbol{C}_p d_p(t) \tag{36}$$

According to the pitch system dynamics described by (16), the lumped disturbance term $d_p(t)$ in (36) is represented as

$$\boldsymbol{C}_p \hat{d}_p(t) = \left(\dot{\boldsymbol{x}}_p - \boldsymbol{A}_p \boldsymbol{x}_p - \boldsymbol{B}_p u\right) * g_f(t) = L^{-1}\left\{G_f(s)\right\} * \left(\dot{\boldsymbol{x}}_p - \boldsymbol{A}_p \boldsymbol{x}_p - \boldsymbol{B}_p u\right) \tag{37}$$

Substituting the disturbance term $d_p(t)$ in (36) with its estimate in (37) yields

$$\boldsymbol{B}_p u = \boldsymbol{A}_m \boldsymbol{x}_p + \boldsymbol{B}_m c(t) - \boldsymbol{A}_p \boldsymbol{x}_p - \boldsymbol{K}_2 \boldsymbol{e}_p(t) - \left(\dot{\boldsymbol{x}}_p - \boldsymbol{A}_p \boldsymbol{x}_p - \boldsymbol{B}_p u\right) * g_f(t) \tag{38}$$

Hence, the UDE based control law is formulated as

$$u = -\boldsymbol{B}_p^{+}\left\{\begin{array}{l} \boldsymbol{A}_p \boldsymbol{x}_p + L^{-1}\left[\dfrac{sG_f(s)}{1-G_f(s)}\right] * \boldsymbol{x}_p + \\ L^{-1}\left[\dfrac{1}{1-G_f(s)}\right]\left(\boldsymbol{A}_m \boldsymbol{x}_p + \boldsymbol{B}_m c(t) - \boldsymbol{K}_2 \boldsymbol{e}_p(t)\right) \end{array}\right\} \tag{39}$$

Substituting (38) into (16) results in

$$\dot{\boldsymbol{x}}_p = \boldsymbol{A}_m \boldsymbol{x}_p + \boldsymbol{B}_m c(t) - \boldsymbol{K}_2 \boldsymbol{e}_p(t) - \boldsymbol{C}_p d_p * g_f(t) + \boldsymbol{C}_p d_p \tag{40}$$

Substituting (34) into (40) and rearranging the resulting equations yields

$$\begin{cases} \boldsymbol{X}_p(s) = \boldsymbol{H}_m(s) C(s) + \boldsymbol{H}_d(s) \boldsymbol{B}_p \boldsymbol{B}_p^{+} \boldsymbol{C}_p \left[1 - G_f(s)\right] d_p \\ \boldsymbol{H}_m(s) = (s\boldsymbol{I} - \boldsymbol{A}_m)^{-1} \boldsymbol{B}_m \\ \boldsymbol{H}_d(s) = \left[1 - G_f(s)\right]\left[s\boldsymbol{I} - (\boldsymbol{A}_m + \boldsymbol{K}_2)\right]^{-1} \end{cases} \tag{41}$$

As revealed in (41), the UDE based pitch angle controller has two-degree-of freedom nature that allows the decoupled design of the reference model and the filter. It is clear that for any bounded uncertain term d_p, if the low-pass filter $G_f(s)$ is chosen to cover the whole frequency content of d_p, the actual state trajectory of the pitch servo system will be only determined by the reference input $c(t)$.

The actual pitch angle tracking error is then obtained by combining (34) and (41) as

$$\boldsymbol{E}_p(s) = -\left[s\boldsymbol{I} - (\boldsymbol{A}_m + \boldsymbol{K}_2)\right]^{-1} \boldsymbol{B}_p \boldsymbol{B}_p^{+} \boldsymbol{C}_p \left[1 - G_f(s)\right] d_p \tag{42}$$

As aforementioned, the low-pass filter $G_f(s)$ is strictly proper and stable with $G_f(0) = 1$, d_p is bounded, and $\left[s\boldsymbol{I} - (\boldsymbol{A}_m + \boldsymbol{K}_2)\right]^{-1}$ is designed to be stable. Then the steady-state error will converge to zero in finite time by applying the final value theorem [20], i.e. $\lim_{t\to\infty} e_p(t) = \lim_{s\to 0} s\boldsymbol{E}_p(s) = 0$. By substituting (27) into (39) and considering (34) and (35), the UDE based control law in (39) is re-formulated as

$$u = -\boldsymbol{B}_p^{+}\left\{\left(\boldsymbol{A}_p + \boldsymbol{A}_m\right)\boldsymbol{x}_m + \boldsymbol{B}_m c(t) + \frac{1}{\tau}\left[\begin{array}{l} \left(2\boldsymbol{x}_m - \boldsymbol{e}_p\right) - \left(\boldsymbol{A}_p + \boldsymbol{A}_m + \boldsymbol{K}_2\right)\tau \boldsymbol{e}_p \\ -\left(\boldsymbol{A}_m + \boldsymbol{K}_2\right)\int_0^t \boldsymbol{e}_p(\xi)\mathrm{d}\xi \end{array}\right]\right\} \tag{43}$$

It is clear that the control law (48) is formulated by using the system state, the reference model, the low-pass filter, and the error feedback gain.

VI. Stability Analysis

The overall stability of the entire tidal pitch angle control system can be analyzed as follows.

For the power smoothing control loop, by using the relationship $\beta = \beta_r - e_\beta$, substituting (33) into the error dynamics (22) and considering (27), the power tracking error dynamics in (22) is re-formulated as

$$\dot{e} = -K_1 e - \tilde{b}\beta + \hat{b}e_\beta - \Delta d \tag{44}$$

where $\Delta d = L^{-1}\left[1 - G_f(s)\right] * d(x,t)$.

For the pitch angle control loop, by considering the estimated lumped disturbance term $d_p(t)$ in (37), the pitch angle tracking error dynamics in (35) becomes

$$\dot{\boldsymbol{e}}_p(t) = (\boldsymbol{A}_m + \boldsymbol{K}_2)\boldsymbol{e}_p(t) - \boldsymbol{C}_p \Delta d_p \tag{45}$$

Define the following Lyapunov function candidates to analyze the stability of the overall tidal pitch control system.

$$\begin{cases} V(t) = V_1(t) + V_2(t); \\ V_1(t) = \dfrac{1}{2}e^2; \\ V_2(t) = \boldsymbol{e}_p^{\mathrm{T}}(t)\boldsymbol{P}\boldsymbol{e}_p(t). \end{cases} \tag{46}$$

Differentiating $V_1(t)$ with respect to time along with the error dynamics in (34) gives

$$\dot{V}_1(t) = e\dot{e} = -K_1 e^2 - e\tilde{b}\beta + e\hat{b}e_\beta - e\Delta d \tag{47}$$

By applying Young's inequality to (47), the following inequality holds.

$$\begin{aligned} \dot{V}_1(t) &\le -K_1 e^2 + \frac{1}{2}e^2 + \frac{1}{2}\left(\hat{b}e_\beta - \tilde{b}\beta - \Delta d\right)^2 \\ &= \left(\frac{1}{2} - K_1\right)e^2 + \frac{1}{2}\left(\hat{b}e_\beta - \tilde{b}\beta - \Delta d\right)^2 \end{aligned} \tag{48}$$

The time derivative of $V_2(t)$ can be obtained as

$$\dot{V}_2(t) = \boldsymbol{e}_p^{\mathrm{T}}(t)\left[(\boldsymbol{A}_m + \boldsymbol{K}_2)^{\mathrm{T}}\boldsymbol{P} + \boldsymbol{P}(\boldsymbol{A}_m + \boldsymbol{K}_2)\right]\boldsymbol{e}_p(t) - 2\boldsymbol{e}_p^{\mathrm{T}}(t)\boldsymbol{P}\boldsymbol{C}_p \Delta d_p \tag{49}$$

By using the following inequalities

$$\begin{cases} \boldsymbol{e}_p^{\mathrm{T}}(t)\left[(\boldsymbol{A}_m + \boldsymbol{K}_2)^{\mathrm{T}}\boldsymbol{P} + \boldsymbol{P}(\boldsymbol{A}_m + \boldsymbol{K}_2)\right]\boldsymbol{e}_p(t) \le \\ \lambda_{\max}\left[(\boldsymbol{A}_m + \boldsymbol{K}_2)^{\mathrm{T}}\boldsymbol{P} + \boldsymbol{P}(\boldsymbol{A}_m + \boldsymbol{K}_2)\right]\boldsymbol{e}_p^{\mathrm{T}}(t)\boldsymbol{e}_p(t) \\ -2\boldsymbol{e}_p^{\mathrm{T}}(t)\boldsymbol{P}\boldsymbol{C}_p \Delta d_p \le \boldsymbol{e}_p^{\mathrm{T}}(t)\boldsymbol{e}_p(t) + \left\|\boldsymbol{P}\boldsymbol{C}_p \Delta d_p\right\|^2 \\ \lambda_{\min}(\boldsymbol{P})\boldsymbol{e}_p^{\mathrm{T}}(t)\boldsymbol{e}_p(t) \le V_2(t) \le \lambda_{\max}(\boldsymbol{P})\boldsymbol{e}_p^{\mathrm{T}}(t)\boldsymbol{e}_p(t) \end{cases} \tag{50}$$

It is natural to derive that

$$\begin{aligned} \dot{V}_2(t) &\le \left\{\lambda_{\max}\left[(\boldsymbol{A}_m + \boldsymbol{K}_2)^{\mathrm{T}}\boldsymbol{P} + \boldsymbol{P}(\boldsymbol{A}_m + \boldsymbol{K}_2)\right] + 1\right\}\boldsymbol{e}_p^{\mathrm{T}}(t)\boldsymbol{e}_p(t) \\ &+ \left\|\boldsymbol{P}\boldsymbol{C}_p \Delta d_p\right\|^2 \le \frac{V_2(t)}{\lambda_{\min}(\boldsymbol{P})}\left\{\lambda_{\max}\left[(\boldsymbol{A}_m + \boldsymbol{K}_2)^{\mathrm{T}}\boldsymbol{P} + \boldsymbol{P}(\boldsymbol{A}_m + \boldsymbol{K}_2)\right] + 1\right\} \\ &+ \left\|\boldsymbol{P}\boldsymbol{C}_p \Delta d_p\right\|^2 \end{aligned} \tag{51}$$

By considering (46), (47) and (51), the time derivative of the Lyapunov function $V(t)$ can be obtained as

$$\dot{V}(t)=\dot{V}_1(t)+\dot{V}_2(t)\le\frac{V_2(t)}{\lambda_{\min}(\boldsymbol{P})}\left\{\lambda_{\max}\left[(\boldsymbol{A}_m+\boldsymbol{K}_2)^{\mathrm{T}}\boldsymbol{P}+\boldsymbol{P}(\boldsymbol{A}_m+\boldsymbol{K}_2)\right]+1\right\}$$
$$+\left\|\boldsymbol{P}\boldsymbol{C}_p\Delta d_p\right\|^2+\left(\frac{1}{2}-K_1\right)e^2+\frac{1}{2}\left(\hat{b}e_\beta-\tilde{b}\beta-\Delta d\right)^2$$
$$\le-(2K_1-1)V_1(t)-$$
$$\left\{-\frac{\left\{\lambda_{\max}\left[(\boldsymbol{A}_m+\boldsymbol{K}_2)^{\mathrm{T}}\boldsymbol{P}+\boldsymbol{P}(\boldsymbol{A}_m+\boldsymbol{K}_2)\right]+1\right\}}{\lambda_{\min}(\boldsymbol{P})}\right\}V_2(t)$$
$$+\left\|\boldsymbol{P}\boldsymbol{C}_p\Delta d_p\right\|^2+\frac{1}{2}\left(\hat{b}e_\beta-\tilde{b}\beta-\Delta d\right)^2 \tag{52}$$

By defining

$$\begin{cases}\gamma_1=\min\left\{(2K_1-1),\ -\dfrac{\left\{\lambda_{\max}\left[(\boldsymbol{A}_m+\boldsymbol{K}_2)^{\mathrm{T}}\boldsymbol{P}+\boldsymbol{P}(\boldsymbol{A}_m+\boldsymbol{K}_2)\right]+1\right\}}{\lambda_{\min}(\boldsymbol{P})}\right\}\\ \gamma_2=\left\|\boldsymbol{P}\boldsymbol{C}_p\Delta d_p\right\|^2+\frac{1}{2}\left(\hat{b}e_\beta-\tilde{b}\beta-\Delta d\right)^2\end{cases} \tag{53}$$

It is natural to derive that

$$\dot{V}(t)=-\gamma_1V(t)+\gamma_2 \tag{54}$$

By solving (54), one obtains

$$0\le V(t)\le V(0)\exp(-\gamma_1t)+\frac{\gamma_2}{\gamma_1}\left[1-\exp(-\gamma_1t)\right] \tag{55}$$

Since γ_1 and γ_2 are positive and bounded due to the local boundness of the pitch angle and the selection of K_1, $\boldsymbol{K}_2$ and $\boldsymbol{P}$, $V(t)$ will be bounded by γ_2/γ_1 when $t\to\infty$. Thus, the power tracking error $e(\infty)<\sqrt{\frac{2\gamma_2}{\gamma_1}}$, which can be readily reduced by increasing the feedback gain K_1 and designing a suitable low pass filter $G_f(s)$ to reduce the estimation errors. Then the closed-loop control system is stable and the asymptotic rated generator power tracking and disturbance rejection is achieved in finite time [19]. We mention that the generator power quality and transient stability may be further improved when considering fault ride-through schemes like wind turbines [21].

VII. Validations and Discussions

In this section, the feasibility and effectiveness of the proposed UDE based power smoothing controller and the pitch angle controller are thoroughly evaluated based on a demonstrative 600 kW tidal turbine with geared transmission and variable pitch control. The proposed tidal pitch system is applicable for general tidal turbines.

The rated tidal stream speed for the pitch angle control is 1.8 m/s. The reference pitch angle is generated by using the control law in (33) and the pitch system is controlled by the UDE based control law in (43). In order to achieve a good attenuation ratio of the UDE control, the time constant τ in the low pass filter $G_f(s)$ is chosen as a small positive value of 0.001 s to ensure that the filter bandwidth covers the spectrum of uncertainties and disturbances. The constant error feedback gain K_1 is chosen to be 0.67, and the error feedback gain matrix $\boldsymbol{K}_2$ is chosen to be diag $\{1.2\times10^3, 1.6\times10^3, 3.4\times10^4\}$. In addition, memory blocks are used to deal with the algebraic loop and unknown power coefficient as mentioned in section IV.

The simulation methods are currently available in Simscape Power Systems™ Specialized Technology in Simulink to model turbine based energy conversion systems. The model is discretized at 5 ms and the dynamics resulting from pitch control system and power system interactions are preserved.

The results of the proposed novel pitch system are compared with that of an existing pitch system [8] to evaluate the generator power qualities and speed control performances under different operation conditions. The control efficiency of the proposed UDE based pitch angle controller is also compared with a conventional Proportional–Integral–Derivative (PID) controller. To compare these two controllers fairly, their parameters are well tuned to produce similar pitch angle tracking performance. The PID parameters are respectively chosen as 4.3×10^8, 0.01 and 1.2×10^5.

A. Pitch System Dynamics

As shown in Fig. 5, the rising time and peak time of the proposed UDE controller are relatively lower than that of the PID controller that is commonly used in most of the commercial wind or tidal turbines. This means that the UDE control responds faster and can help to further improve the pitch system dynamics in comparison with PID control.

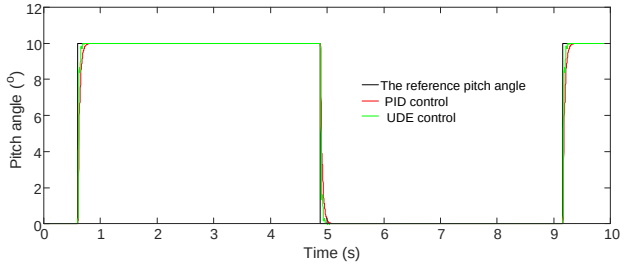

Fig. 5 Responses to the reference square pitch signal

As shown in Fig. 6, the pitch angle tracking errors are almost kept zero by using both the PID and UDE controllers, which indicates that these two controllers can guarantee the stability of the closed-loop pitch servo system. Compared with the PID controller, the UDE based controller maintains lower tracking error and thus better tracking accuracy. This is due to the fact that the UDE controller uses more derivative information than the PID controller.

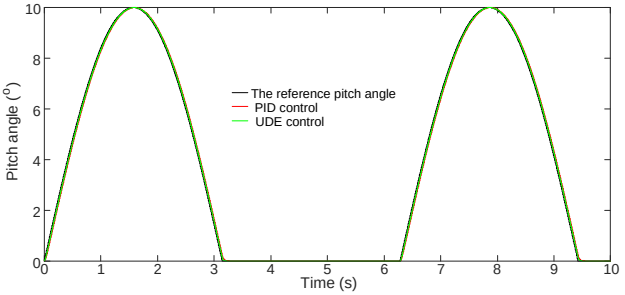

Fig. 6 Responses to the reference sinusoidal pitch signal

B. Pitch Control Performances under Normal Tidal Stream Condition

As shown in Fig. 7, the real-world typical tidal stream speed data (around 1.8 m/s) is used as external input to the tidal turbine system to test the proposed pitch system. The speed signals are of crucial importance to the tidal turbine and

determines its operating regions. Around the tidal speed of 1.8 m/s, the proposed pitch system will be activated to generate suitable pitch angles to smooth generator power. The tidal stream speed can also be accurately approximated by using the speed estimation equations (29)-(31) without using any tidal speed sensors, which will largely reduce system cost.

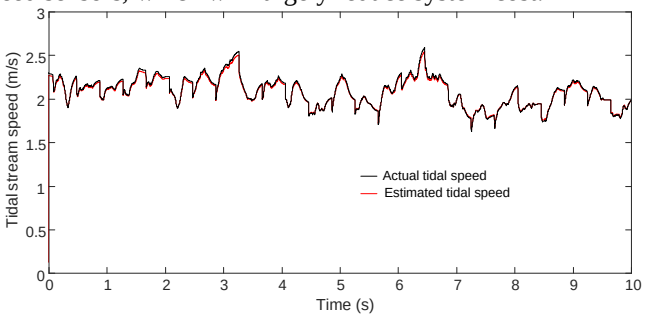

Fig. 7 The tidal stream speed and its estimates

As illustrated in Fig. 8, the two pitch systems are activated during above the rated tidal stream speed conditions to regulate the tidal power generations. The pitch angle from the proposed pitch system varies between 0 and 2.8° while the pitch angle of the existing pitch system [8] varies in a narrower range between 0 and 2.2°. Thus, it is obvious that the proposed pitch system generates pitch angle outputs in a wider range and can therefore execute more pitch actions than the existing pitch system.

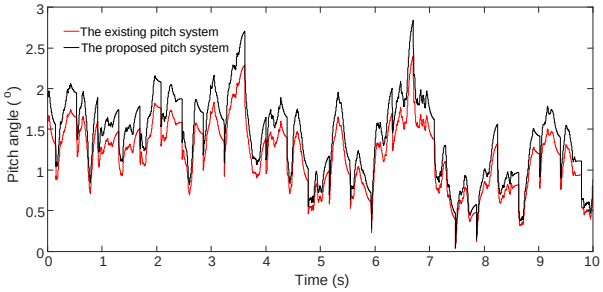

Fig. 8 The pitch angle variations

As shown in Fig. 9, by using the proposed pitch system, the averaged generator power is also smoothed and maintained around the rated value of 600 kW despite of the uncertainty and disturbances from the system dynamics and input signal. On the other hand, the generator power varies more significantly between 500 kW and 700 kW when the existing pitch system is used. This comparison result indicates that the proposed pitch system is more capable of smoothing the generator power and maintaining the rated value than the existing pitch system [8].

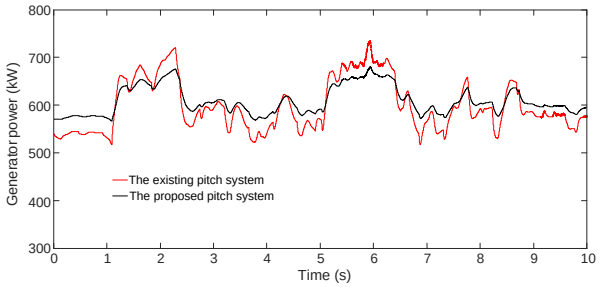

Fig. 9 The generator power variations

C. Pitch Control Performance under Sudden Large Spring Tides

As shown in Fig. 10, the measured real-world sudden large spring tides increases from 0 to around 3.5 m/s which is about two times the rated tidal speed. The extreme speed of 3.5 m/s continues for about 4 s and can be readily used to evaluate the control performances of the proposed pitch system. The estimated tidal stream speed also closely matches the real speed data, which clearly demonstrate the effectiveness of the estimation algorithm in section IV-B.

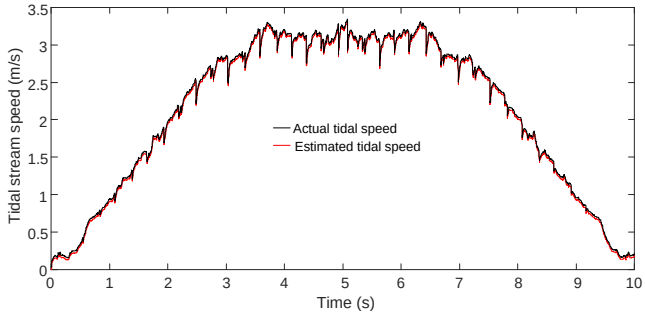

Fig. 10 The tidal stream speed and its estimates

As illustrated in Fig. 11, the pitch angles vary between 0 and 10° and have positive relationship with the tidal stream speed as shown in Fig. 10. The pitch angle generated from the proposed pitch system is relatively larger and varies more significantly than that from the existing pitch system. Therefore, the proposed pitch system is more effective in producing necessary pitch angle control actions to regulate the generator power and speed during the sudden large spring tidal conditions.

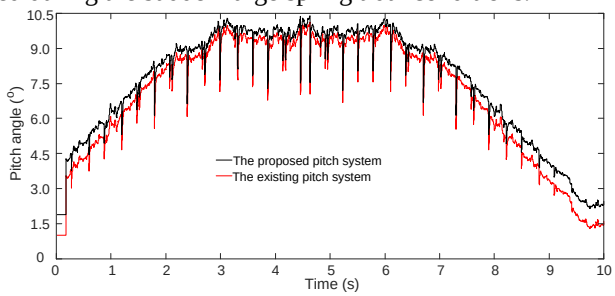

Fig. 11 The pitch angle variations

As shown in Figs. 12 and 13, the generator speed and power suddenly increases to more than 160 rad/s and 750 kW during the sudden large spring tides, causing an oscillation on the DC bus voltage and the grid. During this extreme condition, the pitch systems are timely activated to regulate the generator speed and power at their set points. The generator speed and power can be regulated around the rated values and the fluctuations can be more smoothed when using the proposed pitch system while the generator speed and power fluctuates more significantly when the existing pitch system [8] is applied. This is largely due to the fact that the proposed pitch system has much faster and more accurate pitch control performances as compared with the existing pitch system that has relatively inaccurate pitch actuations due to the inevitably imprecise motion transformations and inherent frictions in the rack and pinion mechanism. As a consequence, the proposed pitch system is more effective in maintaining the rated generator speed and power even in the presence of sudden large spring tides as compared with the existing pitch system.

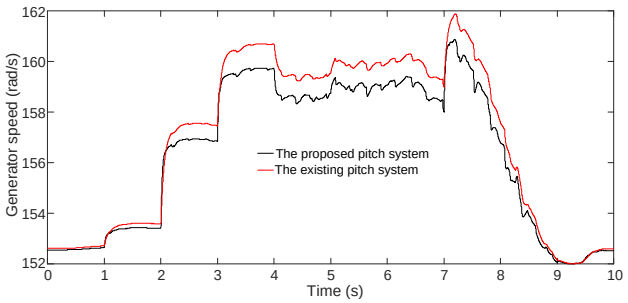

Fig. 12 The generator speed variations

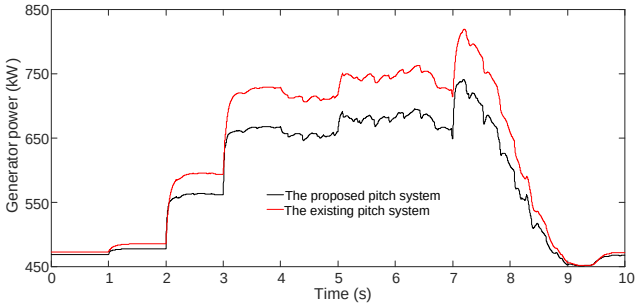

Fig. 13 The generator power variations

As indicated in the aforementioned results, the proposed pitch system can potentially improve tidal energy efficiency and power leveling over a wide range of tidal stream speeds like wind turbine pitch systems [5], [22].

VIII. Conclusion

This paper has presented the systematic design, dynamics modelling and UDE based pitch control of a novel tidal pitch system based on hydraulic servo and bevel geared transmission. The pitch system has compact and triangular structure, and its dynamics model considers model uncertainties and external disturbances that are readily estimated and compensated by the proposed UDE-based control law. The UDE pitch control was designed in a composite hierarchical manner that included an upper level generator power smoothing controller and a low level pitch angle tracking controller. The UDE-based robust power smoothing controller was proposed for accurate and stable operations of the power generation while the UDE based pitch angle controller was designed to have the pitch system to asymptotically track the derived reference pitch angle trajectory. The feasibility and effectiveness of the proposed pitch system and UDE controller have been evaluated through simulation studies based on a 600 kW variable speed, variable pitch tidal turbine. The results demonstrated that the UDE control based pitch system had excellent dynamic characteristics and higher pitch angle tracking accuracy as compared with the conventional PID control method. The proposed tidal pitch system is easy to install on real tidal turbines. Future work is to build an experimental test rig and conduct experiment tests to verify its effectiveness under more complicated situations.

References

[1] Fraenkel P L. Marine current turbines: pioneering the development of marine kinetic energy converters. Proceedings of the Institution of Mechanical Engineers, Part A: Journal of Power and Energy, 2007, 221(2): 159-169.

[2] https://www.atlantisresourcesltd.com/services/turbines/

[3]http://www.all-energy.co.uk/__novadocuments/30405?v=635060457909570000

[4] http://www.reuk.co.uk/wordpress/tidal/lunar-energy-tidal-power/

[5] Duong M Q, Grimaccia F, Leva S, et al. Pitch angle control using hybrid controller for all operating regions of SCIG wind turbine system. Renewable Energy, 2014, 70: 197-203.

[6] Howlader A M, Urasaki N, Yona A, et al. A review of output power smoothing methods for wind energy conversion systems. Renewable and Sustainable Energy Reviews, 2013, 26: 135-146.

[7] Schönborn A, Chantzidakis M. Development of a hydraulic control mechanism for cyclic pitch marine current turbines. Renewable Energy, 2007, 32(4): 662-679.

[8] Gu Y, Lin Y, Xu Q, et al. Blade-pitch system for tidal current turbines with reduced variation pitch control strategy based on tidal current velocity preview. Renewable Energy, 2018, 115: 149-158.

[9] Gu Y, Liu H, Li W, et al. Integrated design and implementation of 120-kW horizontal-axis tidal current energy conversion system. Ocean Engineering, 2018, 158: 338-349.

[10] Whitby B, Ugalde-Loo C E. Performance of pitch and stall regulated tidal stream turbines. IEEE Transactions on Sustainable Energy, 2014, 5(1): 64-72.

[11]http://www.machinedesign.com/linear-motion/go-long-pros-and-cons-rack-and-pinion-systems

[12] Zhong Q C, Kuperman A, Stobart R K. Design of UDE-based controllers from their two‐degree‐of‐freedom nature. International Journal of Robust and Nonlinear Control, 2011, 21(17): 1994-2008.

[13] Zhong Q C, Rees D. Control of uncertain LTI systems based on an uncertainty and disturbance estimator. Journal of dynamic systems, measurement, and control, 2004, 126(4): 905-910.

[14] Stobart R K, Kuperman A, Zhong Q C. Uncertainty and disturbance estimator–based control for uncertain LTI-SISO systems with state delays. Journal of Dynamic Systems, Measurement, and Control, 2011, 133(2): 024502.

[15] Merritt H E. Hydraulic control systems. John Wiley & Sons, 1967.

[16] Yin X, Lin Y, Li W, et al. Design, modeling and implementation of a novel pitch angle control system for wind turbine. Renewable Energy, 2015, 81: 599-608.

[17] Zhong Q C, Wang Y, Ren B. UDE-based robust droop control of inverters in parallel operation. IEEE Transactions on Industrial Electronics, 2017, 64(9): 7552-7562.

[18] Ren B, Zhong Q C, Chen J. Robust control for a class of nonaffine nonlinear systems based on the uncertainty and disturbance estimator. IEEE Transactions on Industrial Electronics, 2015, 62(9): 5881-5888.

[19] Ren B, Zhong Q C, Dai J. Asymptotic reference tracking and disturbance rejection of UDE-based robust control. IEEE Transactions on Industrial Electronics, 2017, 64(4): 3166-3176.

[20] Chen J, Ren B, Zhong Q C. UDE-based trajectory tracking control of piezoelectric stages. IEEE Transactions on Industrial Electronics, 2016, 63(10): 6450-6459.

[21] Duong M Q, Grimaccia F, Leva S, et al. Improving transient stability in a grid-connected squirrel-cage induction generator wind turbine system using a fuzzy logic controller. Energies, 2015, 8(7): 6328-6349.

[22] Senjyu T, Sakamoto R, Urasaki N, et al. Output power leveling of wind turbine generator for all operating regions by pitch angle control. IEEE Transactions on Energy conversion, 2006, 21(2): 467-475.

Xiuxing Yin received his Ph. D. in mechatronic engineering from Zhejiang University, Hangzhou, China in 2016. He is now a research fellow at the University of Warwick, UK. His research interests focus on mechatronics, renewable energy and nonlinear control.

Xiaowei Zhao is Professor of Control Engineering at the University of Warwick. He obtained his PhD degree in Control Theory from Imperial College London, then worked at Oxford University as a postdoc for 3 years before joining Warwick in 2013. His research interests include control and grid integration of renewable energy systems and microgrid, control of fluid-structure interaction, coupled infinite-dimensional systems.